Letter

Viscous resuspension of droplets

Mehdi Maleki, Clément de Loubens,* and Hugues Bodiguel
University of Grenoble Alpes, CNRS, Grenoble INP, LRP, 38000 Grenoble, France

(Received 13 October 2021; accepted 14 January 2022; published 28 January 2022)

Using absorbance measurements through a Couette cell containing an emulsion of buoyant droplets, volume fraction profiles are measured at various shear rates. These viscous resuspension experiments allow a direct determination of the normal stress in the vorticity direction in connection with the suspension balance model that has been developed for suspensions of solid particles. The results unambigously show that the normal viscosity responsible for the shear-induced migration of the droplets is independent on the capillary number, implying that particle deformation does not play a major role. It is similar to that of rigid particles at volume fractions below 40% but much smaller at higher ones.

DOI: 10.1103/PhysRevFluids.7.L011602

Inspired by margination in blood vessels [1–3], there is a growing interest for flow-induced structuration phenomena in suspensions of soft microparticles in order to design cells sorting microfluidic systems for biological analysis [4–6]. Understanding and modeling migration in suspensions of soft particles is considered a veritable challenge because of the nonlinear coupling between hydrodynamic interactions and the dynamics of deformation of the particles [7,8]. In fact, the deformability of the particle is a major ingredient to break the symmetry of inertialess flow. It generates normal forces and particle migration across the streamlines [9,10]. The role of soft lubrication interactions between particles has also been questioned as a collective mechanism of migration [11,12]. Until now, the problem has been addressed by full numerical simulations which consider the interplay among the flow and the dynamics of deformation of the particles and their mechanical properties [8,13–16]. Even in a simple flow, the dynamic of deformation of soft particles is the complex result between the nature of the flow and the mechanical properties of the particle [17,18]. These complex dynamics would seem to play a role in particle migration [19]. In contrast, this paper shows that all these sophisticated details do not need to be considered to account for migration in suspension of particles in a large range of volume fractions and shear rates.

The limiting case of rigid particles, where pair trajectories are perfectly reversible is worth discussion [20,21]. Irreversibility has been discussed to be due to many body hydrodynamic interactions [22–24] but is now recognized to be more likely due to solid frictional contacts between rough particles [20,25–28]. These are thus likely to play a major role in the shear-induced migration observed in heterogeneous flows of suspensions [29,30]. Recent experimental results on viscous resuspension [31,32] support this idea since migration was found to vary nonlinearly with respect to the shear rate, which has been interpreted as a manifestation of non-Coulombian friction. Numerical investigations also highlighted the role of frictional contacts on the rheological properties of suspensions, but only at high volume fraction, since lubrication interactions are dominate for intermediate volume fraction [28,33,34]. The exact role of contact contribution on particle migration thus remains to be clarified and has important theoretical implications [35,36]. When reducing particle stiffness, it is expected that solid contacts between particles will eventually be precluded by

*clement.de-loubens@univ-grenoble-alpes.fr

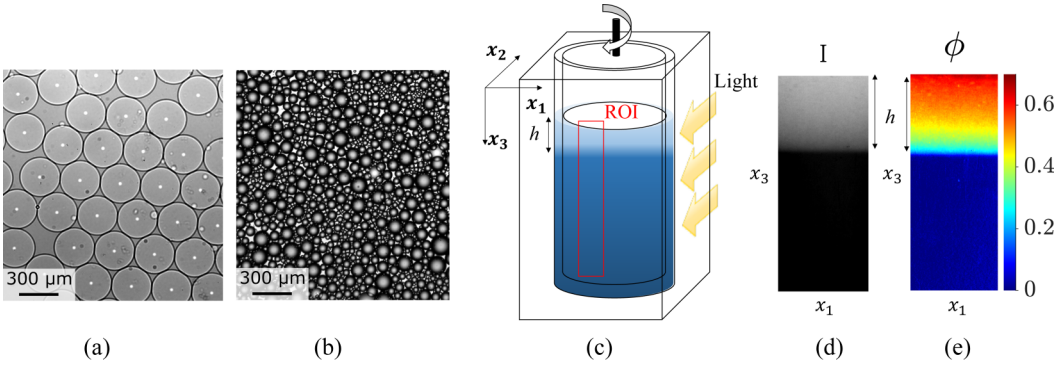

FIG. 1. (a) Monodisperse and (b) polydisperse suspensions of oil-in-water droplets. (c) The suspension was sheared between the two concentric cylinders of a Taylor-Couette cell and visualized by light transmission in the region of interest (ROI) according to $\boldsymbol{x_2}$. h is the height of the resuspended suspension. (d) Transmitted light intensity I in the ROI. (e) Volume fraction of the droplets $\phi \propto \log_{10}(I_0/I)$ in the ROI.

a lubrication film. Therefore, studying shear-induced migration of deformable particles should also shed some lights on its physical origin in suspensions of rigid particles. A transition from a contact driven migration to a deformability driven one could thus be expected. It has been evidenced for pair trajectories [21] but remains to be investigated for suspensions of soft particles.

In order to shed light on the collective mechanisms governing the migration of soft particles, we experimentally studied viscous resuspension of buoyant droplets, which are the simplest model of deformable particles, in a Taylor-Couette geometry, Fig. 1(c). In this configuration, migration occurs in the vorticity direction and is mainly the result of collective interactions between the droplets without interfering with other migration mechanisms such as wall effects and gradients of shear rate. An elegant way of interpreting migration in flow of suspension is to refer to a two-phase momentum balance model, the suspension balance model (SBM) [37,38], which had been developed for rigid particles. The interest of the SBM, compared to diffusive models [39–41], that it connects the particle migration to the suspension rheology. More specifically, the flux of particles is given by a momentum balance between the divergence of the particle stress tensor, buoyancy, and the viscous drag. For rigid particles, constitutive relations among particle stress, volume fraction, and shear rate have been determined [29–32,39,41–44]. For emulsions, earlier theoretical work [45,46] predicted that migration and normal stress depends on both volume fraction and capillary number $\mathrm{Ca} = \eta_0 \dot{\gamma} a/\sigma$ (a being the droplet radius, η_0 the suspending liquid viscosity, and σ the surface tension), which is verified in the dilute case [47]. However, there is a serious lack of experimental data about droplet migration in semidilute regime, despite a few observations suggesting that shear-induced migration in emulsions is effective [48,49]. Here, by filling this gap, we show that the SBM fully accounts for the viscous resuspension in emulsions, and, unexpectedly, that the normal particle stress is linear with respect to the shear rate and independent of Ca, similarly to the rigid case.

Emulsions of non-Brownian droplets were made by dispersing a medium chain triglyceride oil (Nestlé, Switzerland) in an aqueous solution of glycerol (84% w/w, CAS number 56-81-5, VWR) and were stabilized with 1% w/w sorbitan trioleate 85 (CAS number 26266-58-0, Sigma-Aldrich). Monodisperse emulsions were produced with a microfluidic T-junction, radius $a = 143 \pm 5$ μm [Fig. 1(a)], whereas a membrane emulsification device [50,51] (Micropore LDC-1, Micropore Technologies Ltd, UK) was used to produced polydisperse suspensions, $\bar{a} = 47$ μm [Fig. 1(b), see Supplemental Material] [52]. The viscosity and density of both phases were measured with a rotational rheometer (DHR3, TA instruments) and a densimeter (DMA 4500M, Anton Paar) and were $\eta_d = 50$ mPa s, $\eta_c = 85$ mPa s, $\rho_d = 943.42$ kg/m^3, and $\rho_c = 1218.52$ kg/m^3 at 23°C, respectively. The surface tension σ between the two phases was measured by the pendant drop method and was 5 mN/m.

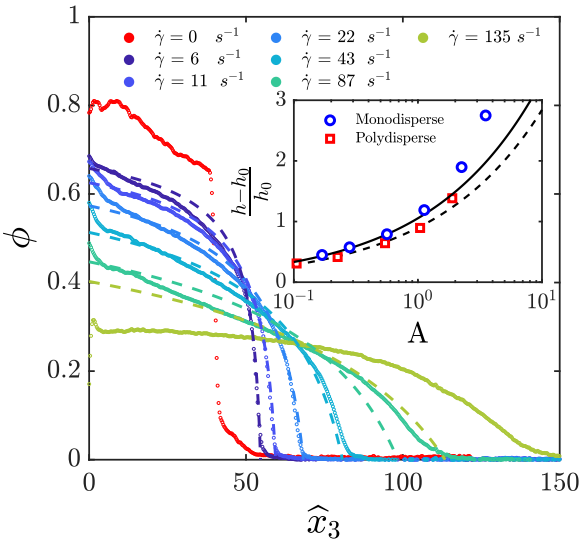

FIG. 2. Steady-state concentration profiles $\phi(\widehat{x}_3)$ for each shear rate step $\dot{\gamma}$ (colored dots) and Eq. (4) with $\phi_m = 0.8$ and $\lambda_3 = 1$ (colored dashed lines) for mono-dispersed suspension. In the insert, the relative height increment of the resuspended layer is plotted as a function of the Acrivos number, $A = a\mathrm{Sh}/h_0$. The solid lines are the SBM predictions.

Resuspension experiments were carried out in a homemade transparent Taylor-Couette cell, 50 mm high and made from PMMA [Fig. 1(c)] driven by a DHR3 rheometer (TA instruments). The inner and outer radii of the cell were $R_1 = 20$ and $R_2 = 24$ mm, respectively. The gap was large enough to accommodate at least 10 droplets, while minimizing the variations of shear rate $\dot{\gamma}$. The suspension of droplets was poured in the cell and left to cream for several hours to obtain a layer of creamed droplets of height h_0. The emulsion was sheared at different increasing steps of $\dot{\gamma}$ from 6 to 260 s^{-1}. For each step, we waited until that the concentration profile reached a steady state. The maximal value of $\dot{\gamma}$ was chosen to keep the Reynolds number $\mathrm{Re} = \rho\Omega R_1(R_2 - R_1)/\eta_0$ sufficiently low to avoid the emergence of Taylor vortices, i.e., $\mathrm{Ta} = \mathrm{Re}^2 2(R_2 - R_1)/(R_1 + R_2) < 900$. It also made it possible to avoid the secondary currents which arise at higher shear rates from the combination of the centrifugal force and buoyancy [31]. This range of shear rate corresponds to a variation of Ca between 10^{-3} and 0.4. Beyond this value, break-up of droplets was expected [53]. To ensure the absence of droplet break-up and/or coalescence, we tested the repeatability of the measurement at the smaller shear rate. Coalescence was furthermore avoided using surface treatment of the cell. Although these precautions were sufficient for the two monodispere emulsions studied, we were only able to limit coalescence for the polydisperse emulsions. However, we quantified it and corrected the h_0 values (see Supplemental Material [52]).

The resuspension process was visualized with a color camera in a region of interest, which was centered along the axis of rotation of the inner cylinder [Fig. 1(c)], see the Supplemental Material [52] for details. The concentration profile $\phi(x_3)$ was inferred by light absorption technique. The optical indexes of both phases of the emulsion were precisely matched. A nonfluorescent colorant (E122, Breton) was added to the continuous phase to provide light absorbance contrast [Fig. 1(d)]. $\phi = KA$ was then inferred from the measurement of the absorbance $A = \log_{10}(I_0/I)$ for each pixel, where I is the light intensity, I_0 the intensity of the background and K the coefficient of attenuation [Figs. 1(d) and 1(e)].

Figure 2 shows the concentration profiles obtained on one of the emulsions used. At rest, the front of ϕ showed a sharp transition between $\phi = 0$ and 0.6. However, contrary to hard spheres, ϕ was not constant in the dense-packed zone and increased from 0.6 to 0.8. It is an indication of

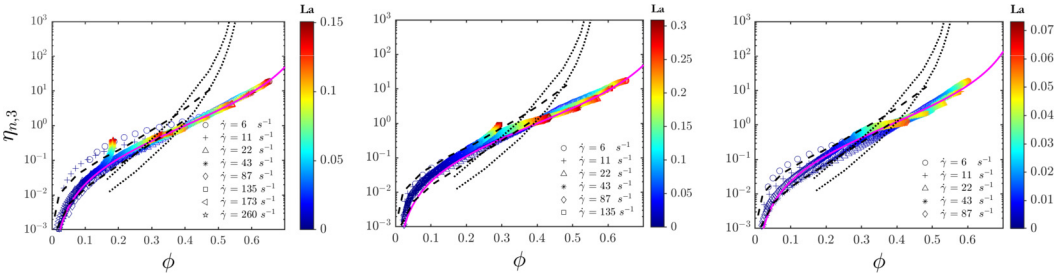

FIG. 3. Relative normal viscosity $\eta_{n,3}$ as a function of the local droplet concentration ϕ for shear rates in the range of $\dot{\gamma} = 6$ to 260 s^{-1}. $\eta_{n,3}$ is inferred by integration of the concentration profile, Eq. (2). The solid lines are the best fit of Eq. (1) (using $n = 2$). Left: Monodisperse emulsion with $a = 185$ μm, $h_0 = 3.6$ mm, $\phi_m = 0.8$, and $\lambda_3 = 1$. Middle: Monodisperse emulsion with $a = 143$ μm, $h_0 = 5.4$ mm, $\phi_m = 0.8$, and $\lambda_3 = 1$. Right: Polydisperse emulsion with $\overline{a} = 47$ μm, $h_0 = 4$ to 6 mm, $\phi_m = 0.76$, and $\lambda_3 = 0.69$. The color represents the Laplace number which denotes particle deformation. The dashed and dotted lines correspond to the experimental results on rigid particles of Refs. [31] and [32], respectively.

droplets deformation, because the droplets at the top of the layer underwent the hydrostatic pressure of the layers below [54]. We defined a local Laplace number La, as the ratio of this pressure over the Laplace pressure, i.e., $\mathrm{La} = a \int \phi \Delta\rho g dz/\sigma$ and showed (see Supplemental Material [52]) that ϕ is, at rest, a unique function of La up to 0.3.

The increasing shear rate $\dot{\gamma}$, the height h of the suspended layer increased as the mean value of ϕ decreased, due to volume conservation. Integration of ϕ showed that the volume of droplets was conserved throughout the experiment, which validated its measurement (see Supplemental Material [52]). In the SBM framework, the steady-state volume fraction profiles result from the momentum balance in the particle phase, i.e., $\phi\Delta\rho g + \nabla \cdot \mathbf{\Sigma}_p$. Under the hypothesis of linearity with respect to the shear rate, the particle normal stress could be written as $\Sigma_{p,ii} = \eta_0 \eta_{n,i}(\phi)|\dot{\gamma}|$ where η_n is the nondimensional normal viscosity [37,38]. If the momentum balance is simplified, then we easily obtain

$$\frac{\phi}{\mathrm{Sh}} = -\frac{d\eta_{n,3}}{d\phi}\frac{d\phi}{d\widehat{x}_3}, \tag{1}$$

where $\widehat{x}_3 = x_3/a$ and $\mathrm{Sh} = \eta_0\dot{\gamma}/\Delta\rho g a$ is the Shields number. Thus, integrating Eq. (1) along the resuspended height provides a measurement of $\eta_{n,3}$ over a range of ϕ which depends on Sh (or $\dot{\gamma}$),

$$\eta_{n,3} = \frac{1}{\mathrm{Sh}} \int_{\widehat{x}_3}^{h/a} \phi(u) du. \tag{2}$$

The results of this integration are presented in Fig. 3. Unambiguously, most of the data fall on the same master curve. Deviations observed for the smallest shear rates at low ϕ are not relevant since the corresponding volume fraction profiles tend toward zero very sharply, over a distance that is about the size of a droplet. For the highest shear rates, a small deviation could also be seen at the very top of the resuspended layer. It can have several origins (contribution of Ca, inertia, radial migration).

For rigid particles, the normal viscosity is given by

$$\eta_{n,i} = \lambda_i \phi^n (1 - \phi/\phi_m)^{-n}, \tag{3}$$

where λ_i are anisotropy coefficients, ϕ_m the maximal volume fraction, and the exponent n has been found to be 2 [30,31,38] or 3 [32,43]). The evolution of $\eta_{n,3}(\phi)$ is very well fitted by Eq. (3) with $n = 2$. The validity of these fits was also tested directly on $\phi(\widehat{x}_3)$ which are more sensitive to the

values of the coefficients. For $n = 2$, the concentration profile is given by [31]

$$\frac{\phi(\widehat{x}_3)}{\phi_m} = 1 - \left[1 + \frac{\phi_m}{\lambda_3 \mathrm{Sh}}(\widehat{h} - \widehat{x}_3)\right]^{-1/2}, \tag{4}$$

where the normalized height of the suspension in the steady state $\widehat{h}$ is

$$\widehat{h} = \widehat{h}_0 + 2\sqrt{\frac{\lambda_3 \widehat{h}_0}{\phi_m}}\mathrm{Sh}. \tag{5}$$

The experimental and analytical profiles of $\phi(\widehat{x}_3)$ are in very good agreement (see Fig. 2 and Supplemental Material [52]), except for the highest value of $\dot{\gamma}$. The relative height increments (insert in Fig. 2) also show a very good agreement with Eq. (5).

These results shows that a simple constitutive equation of $\eta_{n,3}$ for a suspension of deformable droplets is sufficient to catch migration phenomena without further sophistication of the SBM. Strikingly, even when droplet deformation cannot be neglected at rest, i.e., for Laplace number above 0.05, it does not affect the normal viscosity under shear up to La $\sim$ 0.3. The linear dependency with respect to the shear rate rules out some significant contribution of migration mechanisms due to drop deformability in the vorticity direction. This result is consistent with some simulation results showing a weak dependence of the normal forces when varying Ca [55].

The polydisperse emulsion exhibited a very similar behavior, with only small differences in the coefficients. This result is rather surprising as some size segregation of the droplet under shear could be expected. Our results indicate this kind of behavior does not affect the macroscopic particle viscosity or the maximal volume fraction.

The main difference with rigid particles concerns the value of ϕ_m which is comprised between 0.53 and 0.63, whereas it is 0.8 for the emulsions. As highlighted in Fig. 3, the particle normal viscosity is therefore much higher for rigid ones than for droplets when $\phi > 0.4$. At these volume fractions, frictional contacts dominate the rheology of rigid ones [34], whereas droplets are likely to be frictionless.

Let us now discuss the dynamics of resuspension. Momentum balance in the direction x_3 and mass conservation of the particulate phase read

$$\frac{\partial \Sigma_{p,33}}{\partial x_3} - \frac{9}{2}\frac{\eta_0}{a^2}\frac{\phi}{f(\phi)}(u_{p,3} - u_3) + \Delta\rho g\phi = 0, \tag{6}$$

$$\frac{\partial \phi}{\partial t} + \frac{\partial \phi u_{p,3}}{\partial x_3} = 0, \tag{7}$$

where u_p and u are the velocities of the particle phase and suspension phase, respectively. The second term in Eq. (7) corresponds to the viscous drag on the particle phase. f is the hindered settling factor which is given by $(1 - \phi)^5$ [56]. For suspensions of droplets, f also depends on the viscosity ratio between the dispersed and continuous phases κ. Several expressions were proposed in Zinchenko *et al.* [57] and Ramachandran *et al.* [46] in the limit of small ϕ and Ca. The simplest expression was $f_0 = (2\kappa + 2)/(9\kappa + 6)$. We extend their results finite values of ϕ and Ca by writing $f = f_0(1 - \phi)^5$. The system of Eq. (7) was solved for $u_3 = 0$ and using the normal viscosity determined in steady state. They are compared to the experimental results shown in Fig. 4. An excellent agreement is found for monodisperse emulsions. In the range of parameters investigated, the kinetics is governed by a single characteristic time, $\tau = \eta_0 h_0/\Delta\rho g a^2$, and does not significantly depend on the shear rate. For the polydisperse case, the kintetics is about two times faster, but this is not surprising as it is very sensitive to the particle size.

We conclude that the SBM quantitatively accounts for the viscous resuspension of droplets. Moreover, the particle normal stress is linear with respect to the shear rate and proportional to $\phi^2/(1 - \phi/\phi_m)^2$, similarly to rigid particles but with a higher maximal volume fraction. This result has important consequences. The first is the role of the droplet deformability. The normal stress,

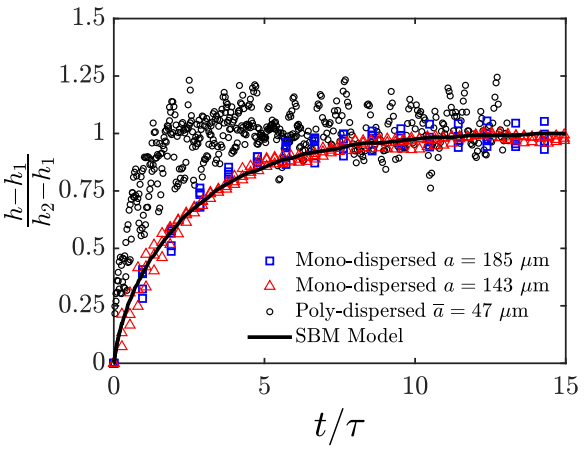

FIG. 4. Variation of the total height h of resuspended layer, when the shear rate is suddenly changed from $\dot{\gamma}_1$ to $\dot{\gamma}_2$. The corresponding steady-state heights are h_1 and h_2, respectively. The time is normalized by $\tau = \eta_0 h_0/\Delta\rho g a^2$. Several experiments are plotted together for each system ($\dot{\gamma}$ ranges from 10 and 100 s^{-1}) and collapse on a single curve. The solid lines are the calculated solutions of the SBM (see text).

which is in principle a function of ϕ and Ca, does not depend on Ca up to 0.4. This implies that in the vorticity direction collective effects prevails over the coupling between particle shape and flow. The second consequence relates to the role of contact forces in shear-induced migration of particles. Leaving aside the small shear-thinning that has recently been reported for suspension of rigid particles [31,32], it is striking to observe that switching from rigid particles where frictional contacts dominate the rheology at high volume fractions, to droplets which could be considered as a frictionless particles, the normal stress is greatly reduced for $\phi > 40\%$. This highlights the crucial role of frictional contacts in dense suspensions. Outlooks of this work deal with size segregation that should occur is the polydisperse case.

Laboratoire Rhéologie et Procédés (LRP) is part of the LabEx Tec21 (ANR-11-LABX-0030) and of the PolyNat Carnot Institute (ANR-11-CARN-007-01). The authors acknowledge funding from University of Grenoble Alpes and from ANR (ANR-17-CE7-0040).

[1] R. Fahraeus and T. Lindqvist, The viscosity of the blood in narrow capillary tubes, Am. J. Physiol. **96**, 562 (1931).
[2] L. L. Munn and M. M. Dupin, Blood cell interactions and segregation in flow, Ann. Biomed. Eng. **36**, 534 (2008).
[3] A. R. Pries, T. W. Secomb, P. Gaehtgens, and J. Gross, Blood flow in microvascular networks: Experiments and simulation, Circ. Res. **67**, 826 (1990).
[4] H. L. Goldsmith and S. Spain, Margination of leukocytes in blood flow through small tubes, Microvasc. Res. **27**, 204 (1984).
[5] S. S. Shevkoplyas, T. Yoshida, L. L. Munn, and M. W. Bitensky, Biomimetic autoseparation of leukocytes from whole blood in a microfluidic device, Anal. Chem. **77**, 933 (2005).
[6] E. Henry, S. H. Holm, Z. Zhang, J. P. Beech, J. O. Tegenfeldt, D. A. Fedosov, and G. Gompper, Sorting cells by their dynamical properties, Sci. Rep. **6**, 34375 (2016).
[7] A. Kumar and M. D. Graham, Margination and segregation in confined flows of blood and other multicomponent suspensions, Soft Matter **8**, 10536 (2012).
[8] J. B. Freund, Numerical simulation of flowing blood cells, Annu. Rev. Fluid Mech. **46**, 67 (2014).

[9] N. Callens, C. Minetti, G. Coupier, M.-A. Mader, F. Dubois, C. Misbah, and T. Podgorski, Hydrodynamic lift of vesicles under shear flow in microgravity, Europhys. Lett. **83**, 24002 (2008).
[10] B. Kaoui, G. H. Ristow, I. Cantat, C. Misbah, and W. Zimmermann, Lateral migration of a two-dimensional vesicle in unbounded poiseuille flow, Phys. Rev. E **77**, 021903 (2008).
[11] P.-Y. Gires, A. Srivastav, C. Misbah, T. Podgorski, and G. Coupier, Pairwise hydrodynamic interactions and diffusion in a vesicle suspension, Phys. Fluids **26**, 013304 (2014).
[12] X. Grandchamp, G. Coupier, A. Srivastav, C. Minetti, and T. Podgorski, Lift and Down-Gradient Shear-Induced Diffusion in Red Blood Cell Suspensions, Phys. Rev. Lett. **110**, 108101 (2013).
[13] P. Bagchi and R. M. Kalluri, Rheology of a dilute suspension of liquid-filled elastic capsules, Phys. Rev. E **81**, 056320 (2010).
[14] J. R. Clausen, D. A. Reasor, and C. K. Aidun, The rheology and microstructure of concentrated noncolloidal suspensions of deformable capsules, J. Fluid Mech. **685**, 202 (2011).
[15] H. Zhao, E. S. Shaqfeh, and V. Narsimhan, Shear-induced particle migration and margination in a cellular suspension, Phys. Fluids **24**, 011902 (2012).
[16] D. A. Fedosov and G. Gompper, White blood cell margination in microcirculation, Soft Matter **10**, 2961 (2014).
[17] J. Deschamps, V. Kantsler, and V. Steinberg, Phase Diagram of Single Vesicle Dynamical States in Shear Flow, Phys. Rev. Lett. **102**, 118105 (2009).
[18] C. de Loubens, J. Deschamps, F. Edwards-Levy, and M. Leonetti, Tank-treading of microcapsules in shear flow, J. Fluid Mech. **789**, 750 (2016).
[19] A. R. Malipeddi and K. Sarkar, Shear-induced gradient diffusivity of a red blood cell suspension: Effects of cell dynamics from tumbling to tank-treading, Soft Matter **17**, 8523 (2021).
[20] F. Da Cunha and E. Hinch, Shear-induced dispersion in a dilute suspension of rough spheres, J. Fluid Mech. **309**, 211 (1996).
[21] W. Chèvremont, H. Bodiguel, and B. Chareyre, Lubricated contact model for numerical simulations of suspensions, Powder Technol. **372**, 600 (2020).
[22] M. Marchioro and A. Acrivos, Shear-induced particle diffusivities from numerical simulations, J. Fluid Mech. **443**, 101 (2001).
[23] A. Sierou and J. F. Brady, Shear-induced self-diffusion in non-colloidal suspensions, J. Fluid Mech. **506**, 285 (2004).
[24] D. J. Pine, J. P. Gollub, J. F. Brady, and A. M. Leshansky, Chaos and threshold for irreversibility in sheared suspensions, Nature (Lond.) **438**, 997 (2005).
[25] M. Popova, P. Vorobieff, M. S. Ingber, and A. L. Graham, Interaction of two particles in a shear flow, Phys. Rev. E **75**, 066309 (2007).
[26] F. Blanc, F. Peters, and E. Lemaire, Experimental Signature of the Pair Trajectories of Rough Spheres in the Shear-Induced Microstructure in Noncolloidal Suspensions, Phys. Rev. Lett. **107**, 208302 (2011).
[27] P. Pham, B. Metzger, and J. E. Butler, Particle dispersion in sheared suspensions: Crucial role of solid-solid contacts, Phys. Fluids **27**, 051701 (2015).
[28] S. Gallier, E. Lemaire, F. Peters, and L. Lobry, Rheology of sheared suspensions of rough frictional particles, J. Fluid Mech. **757**, 514 (2014).
[29] M. Lyon and L. Leal, An experimental study of the motion of concentrated suspensions in two-dimensional channel flow. Part 1. Monodisperse systems, J. Fluid Mech. **363**, 25 (1998).
[30] F. Boyer, O. Pouliquen, and É. Guazzelli, Dense suspensions in rotating-rod flows: Normal stresses and particle migration, J. Fluid Mech. **686**, 5 (2011).
[31] B. Saint-Michel, S. Manneville, S. Meeker, G. Ovarlez, and H. Bodiguel, X-ray radiography of viscous resuspension, Phys. Fluids **31**, 103301 (2019).
[32] E. d'Ambrosio, F. Blanc, and E. Lemaire, Viscous resuspension of non-brownian particles: Determination of the concentration profiles and particle normal stresses, J. Fluid Mech. **911**, A22 (2021).
[33] R. Mari, R. Seto, J. F. Morris, and M. M. Denn, Shear thickening, frictionless and frictional rheologies in non-brownian suspensions, J. Rheol. **58**, 1693 (2014).

[34] W. Chèvremont, B. Chareyre, and H. Bodiguel, Quantitative study of the rheology of frictional suspensions: Influence of friction coefficient in a large range of viscous numbers, Phys. Rev. Fluids **4**, 064302 (2019).
[35] D. Lhuillier, Migration of rigid particles in non-brownian viscous suspensions, Phys. Fluids **21**, 023302 (2009).
[36] P. R. Nott, E. Guazzelli, and O. Pouliquen, The suspension balance model revisited, Phys. Fluids **23**, 043304 (2011).
[37] P. R. Nott and J. F. Brady, Pressure-driven flow of suspensions: Simulation and theory, J. Fluid Mech. **275**, 157 (1994).
[38] J. F. Morris and F. Boulay, Curvilinear flows of noncolloidal suspensions: The role of normal stresses, J. Rheol. **43**, 1213 (1999).
[39] D. Leighton and A. Acrivos, Viscous resuspension, Chem. Eng. Sci. **41**, 1377 (1986).
[40] R. J. Phillips, R. C. Armstrong, R. A. Brown, A. L. Graham, and J. R. Abbott, A constitutive equation for concentrated suspensions that accounts for shear-induced particle migration, Phys. Fluids **4**, 30 (1992).
[41] A. Acrivos, R. Mauri, and X. Fan, Shear-induced resuspension in a couette device, Int. J. Multiphase Flow **19**, 797 (1993).
[42] B. Snook, J. E. Butler, and É. Guazzelli, Dynamics of shear-induced migration of spherical particles in oscillatory pipe flow, J. Fluid Mech. **786**, 128 (2016).
[43] I. E. Zarraga, D. A. Hill, and D. T. Leighton Jr., The characterization of the total stress of concentrated suspensions of noncolloidal spheres in newtonian fluids, J. Rheol. **44**, 185 (2000).
[44] F. Boyer, É. Guazzelli, and O. Pouliquen, Unifying Suspension and Granular Rheology, Phys. Rev. Lett. **107**, 188301 (2011).
[45] W. Schowalter, C. Chaffey, and H. Brenner, Rheological behavior of a dilute emulsion, J. Colloid Interface Sci. **26**, 152 (1968).
[46] A. Ramachandran, M. Loewenberg, and D. T. Leighton, Jr., A constitutive equation for droplet distribution in unidirectional flows of dilute emulsions for low capillary numbers, Phys. Fluids **22**, 083301 (2010).
[47] M. R. King and D. T. Leighton, Jr., Measurement of shear-induced dispersion in a dilute emulsion, Phys. Fluids **13**, 397 (2001).
[48] K. Hollingsworth and M. Johns, Droplet migration in emulsion systems measured using mr methods, J. Colloid Interface Sci. **296**, 700 (2006).
[49] M. Abbas, A. Pouplin, O. Masbernat, A. Liné, and S. Décarre, Pipe flow of a dense emulsion: Homogeneous shear-thinning or shear-induced migration? AIChE J. **63**, 5182 (2017).
[50] S. R. Kosvintsev, G. Gasparini, R. G. Holdich, I. W. Cumming, and M. T. Stillwell, Liquid- liquid membrane dispersion in a stirred cell with and without controlled shear, Ind. Eng. Chem. Res. **44**, 9323 (2005).
[51] M. Maleki, C. de Loubens, K. Xie, E. Talansier, H. Bodiguel, and M. Leonetti, Membrane emulsification for the production of suspensions of uniform microcapsules with tunable mechanical properties, Chem. Eng. Sci. **237**, 116567 (2021).
[52] See Supplemental Material at http://link.aps.org/supplemental/10.1103/PhysRevFluids.7.L011602 for experimental details.
[53] B. Bentley and L. G. Leal, An experimental investigation of drop deformation and breakup in steady, two-dimensional linear flows, J. Fluid Mech. **167**, 241 (1986).
[54] M. Henschke, L. H. Schlieper, and A. Pfennig, Determination of a coalescence parameter from batch-settling experiments, Chem. Eng. J. **85**, 369 (2002).
[55] O. Aouane, A. Scagliarini, and J. Harting, Structure and rheology of suspensions of spherical strain-hardening capsules, J. Fluid Mech. **911**, A11 (2021).
[56] J. Richardson and W. Zaki, Sedimentation and fluidisation: Part i, Chem. Eng. Res. Des **75**, S82 (1997).
[57] A. Zinchenko, Effect of hydrodynamic interactions between the particles on the rheological properties of dilute emulsions, J. Appl. Math. Mech. **48**, 198 (1984).